

Contents

1. Introduction
2. Fluids
- 3. Physics of Microfluidic Systems**
4. Microfabrication Technologies
5. Flow Control
6. Micropumps
7. Sensors
8. Ink-Jet Technology
9. Liquid Handling
10. Microarrays
11. Microreactors
12. Analytical Chips
13. Particle-Laden Fluids
 - a. Measurement Techniques
 - b. Fundamentals of Biotechnology
 - c. High-Throughput Screening

3. Physics of Microfluidic Systems

3.1. Navier-Stokes Equations

3.2. Laminar and Turbulent Flow

3.3. Fluid Dynamics

3.4. Fluidic Networks

3.5. Energy Transport

3.6. Interfacial Surface Tension

3.7. Electrokinetics

3.7. Electrokinetics

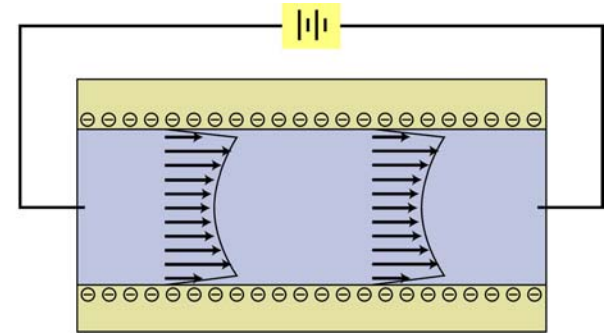
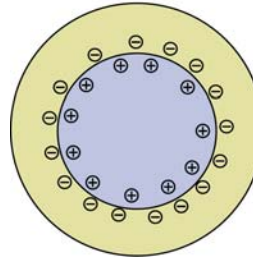
- Topics of electrokinetics (EK)

- Electroosmosis (EO)

- Surface charges

- Electrophoresis (EP)

- Ionic charges in liquid bulk



- Electrophoretic separations

- Both phenomena observed simultaneously

- Suppression of electroosmosis

- Surface modification
- Buffer solutions (pH)

- Microfluidic devices

- Often controlled by EK

3.7. History of Electrokinetics

- Reuss in 1808
 - DC applied to clay-water mixture
 - First observation of EK effect
- Napier in 1846
 - Distinction between EO and EP
- Quincke in 1861
- Helmholtz in 1879
 - Analytical model
- Pellat (1904) and Smoluchowski (1921)
 - Extension of Helmholtz model to derive EK velocity
- Leo Casagrande (1941)
 - EK phenomena in porous media like soils



H. Helmholtz

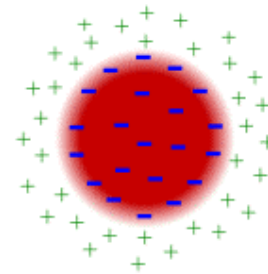
3.7. Electrokinetics

1. Electric Double Layers

2. Electroosmotic Flow

3. Electrophoresis

4. Dielectrophoresis



3.7.1. Electric Double Layers (EDLs)

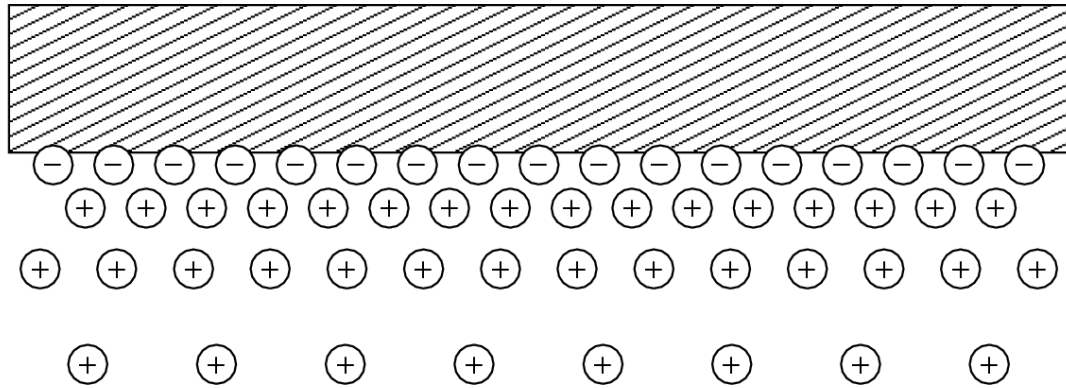


Fig. 3.39. Electric double layers forming on a solid-liquid interface

- Surface charges
 - Keystone for EK
 - Release of **free energy** $G = H - TS$ at interface
 - E.g., dissociation of ions or ionic groups
 - Deprotonation of silanol group



- Thermodynamic equilibrium
 - Layer of immobilized charges
 - **Charge density** σ_q governed by **pH-value**

3.7.1. EDL-Structure and Surface Potential

- Reaction of liquid
 - Screening of immobilized charges
 - Surplus of oppositely charged liquid molecules at interface
 - Capacitive coupling
 - Counteracting Brownian motion (diffusion)

- Potential in EDL
 - Poisson equation
 - Charge density ρ_q

$$\Delta \psi = \frac{\rho_q}{\epsilon \epsilon_0}$$

- Helmholtz-model for EDL
 - Rigid double layer of atomic dimension
 - One-by-one matching of charges
 - Linear decrease of potential in intermediate region

3.1.1. Gouy-Chapman Model

- **Diffusion** counteracts rigid „Helmholtz“-alignment

- Poisson-Boltzmann equation

- Assumption

- Point-like ions
- Undisturbed dielectric constant ε of solvent

$$\rho_q(x) = \rho_{q,0} \exp \left[-\frac{ze\psi(x)}{k_B T} \right]$$

- Radial charge-density distribution

- Debye length

$$r_D = \sqrt{\frac{\varepsilon \varepsilon_0 k_B T}{e^2 \sum_i c_i z_i^2}}$$

$$\rho_q(r) = -\frac{\varepsilon \varepsilon_0}{r_D^2} \zeta \frac{I_0(r/r_D)}{I_0(r_0/r_D)}$$

- Charge density σ_q at surface

- ζ - potential ~ 0.1 V

$$\sigma_q = \frac{\varepsilon \varepsilon_0 \zeta}{r_D}$$

3.1.1. Stern Model

- Helmholtz model
 - High concentration limit
- Gouy-Chapman model
 - High dilution limit
- Interpolation
 - Stern plane at $x = \delta$
 - Reflecting finite size of ions
 - Thickness on nanometer-scale
 - Molecular condenser
 - Stern layer
 - Bulk liquid
- Thermodynamic equilibrium
 - Surface potential attracts ions from bulk
 - Energy required for dehydration process near surface
 - Brownian motion

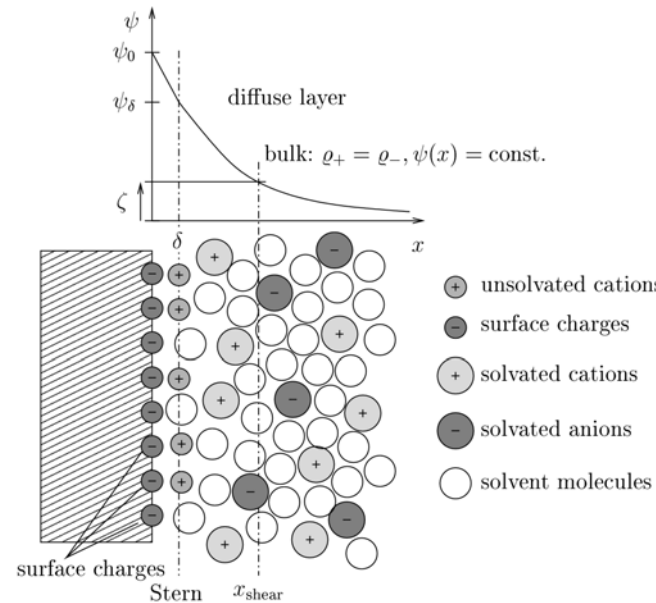


Fig. 3.40. Structure of the first fluid layers next to a (negatively) charged surface. The curve of the surface potential $\psi(x)$ reflects the transition from the surface over the immobilized Stern plane at $x = \delta$ and the diffuse layer to the bulk solution with $\psi(x \rightarrow \infty) = 0$

3.7.1. Stern Model

- Stern layer
 - Specifically bound molecules
 - Inner Helmholtz layer
 - Partially solvated ions
 - Outer Helmholtz layer
 - Completely solvated ions
 - Both layers very narrow
 - On range of atomic dimensions

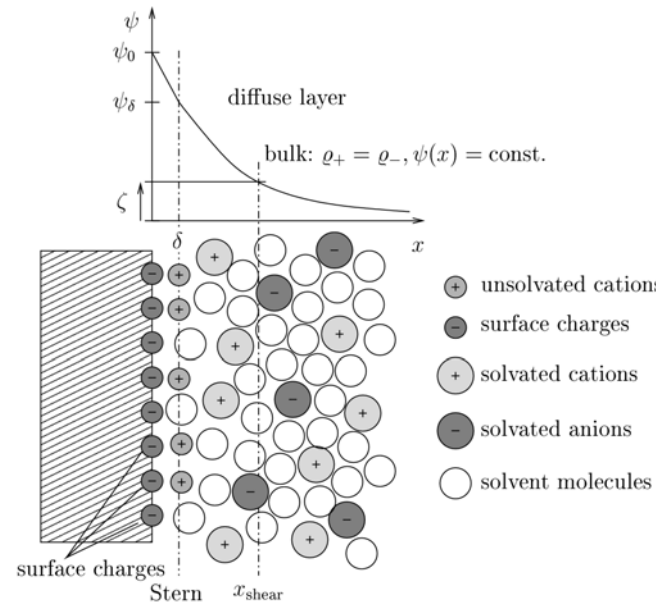


Fig. 3.40. Structure of the first fluid layers next to a (negatively) charged surface. The curve of the surface potential $\psi(x)$ reflects the transition from the surface over the immobilized Stern plane at $x = \delta$ and the diffuse layer to the bulk solution with $\psi(x \rightarrow \infty) = 0$

- Diffuse layer
 - Kinetic energy of same magnitude as electrostatic potential
 - Approximation of point charges justified
 - Brownian motion
 - Exponential decay of potential

3.7.1. Zeta-Potential

- Pressure-driven flow
 - Formation of shear plane
 - Located beyond Stern plane at $x = \delta$

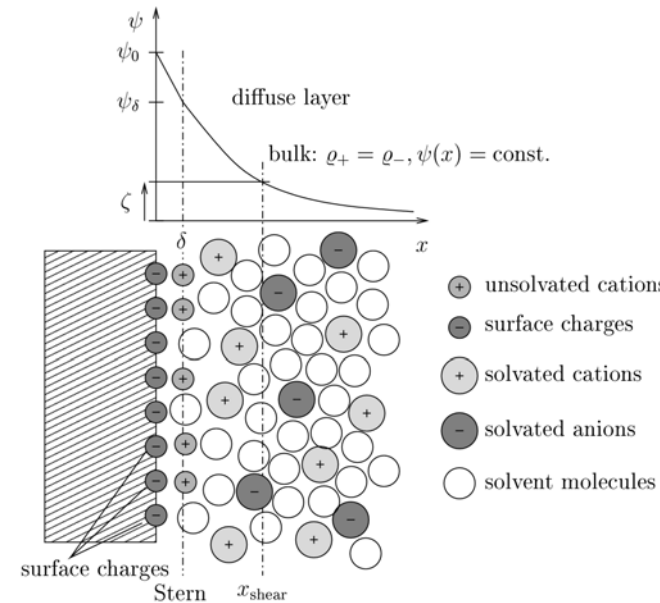


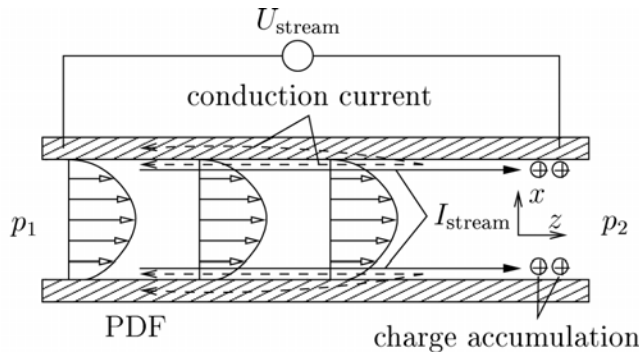
Fig. 3.40. Structure of the first fluid layers next to a (negatively) charged surface. The curve of the surface potential $\psi(x)$ reflects the transition from the surface over the immobilized Stern plane at $x = \delta$ and the diffuse layer to the bulk solution with $\psi(x \rightarrow \infty) = 0$

$$\zeta = \psi(x_{\text{shear}}) - \psi(x \mapsto \infty)$$

3.7.1. Electric Double Layers

- Heat transfer
 - Pinning of liquid molecules in EDL
 - Blocking of diffusive heat transport
 - Nu increases with decreasing ζ -potential

3.7.1. Streaming Current



Hydrodynamic -> Electric

$$I_{\text{stream}} = \int_A \mathbf{v}(\mathbf{r}) \rho_q(\mathbf{r}) d\mathbf{A}$$

Fig. 3.41. Streaming potential U_{stream} and current I_{stream} in a pressure-driven flow (PDF). Charges from the EDL are dragged in the direction of the PDF constituting a charge flow I_{stream} . Due to charge accumulation and depletion at the ends of capillary, a streaming potential U_{stream} forms. U_{stream} in turn initiates a conduction current through the wall or the liquid, depending on the conductivities of the media

- PDF
 - Displacement of charge in shear plane
- Streaming current
 - Counteracting flow through
 - Liquid (ions)
 - Wall (electrons)
 - Wetted perimeter w

$$v_{\text{shear}} = v(x_{\text{shear}} - r_D < x < x_{\text{shear}} + r_D) \simeq \left. \frac{\partial v_z}{\partial x} \right|_{x_{\text{shear}}} r_D$$

$$v_{\text{shear}} = \frac{dr_D \Delta p}{\eta l}$$

$$I_{\text{stream}} = \sigma_{q,\text{shear}} w v_{\text{shear}} = \frac{w \sigma_{q,\text{shear}} dr_D \Delta p}{\eta l}$$

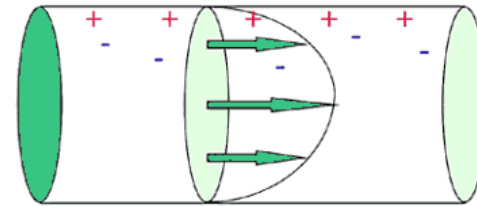
3.7.1. Streaming Potential

- Streaming current I_{stream}
 - Charge displacement
 - Counteracting potential
- Streaming potential U_{stream}
 - Conversion
 - Mechanical force Δp
 - Electric potential U
 - Powering I_{stream}
 - Helmholtz-Smoluchowski
 - Between parallel plates
 - Gap distance d
 - Electric resistance R
 - Electrolyte
 - Channel wall

Hydrodynamic -> Electric

Applied pressure induces flow

Stern double layer



Resultant electric potential via charge separation

Poiseuille flow

$$U_{\text{stream}} = \frac{\zeta \epsilon \epsilon_0 w d R \Delta p}{\eta l}$$

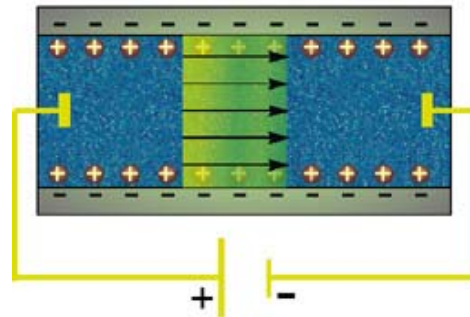
3.7.1. Electric Double Layers

- Electroviscous effect
 - Streaming current powered by mechanical force
 - Hydrodynamic effect similar to viscosity
 - Apparent viscosity > bulk viscosity
 - Thickness of EDL however small (nm to μm)
 - Effect only important for small-diameter tubes

3.7. Electrokinetics

1. Electric Double Layers
- 2. Electroosmotic Flow**
3. Electrophoresis
4. Dielectrophoresis

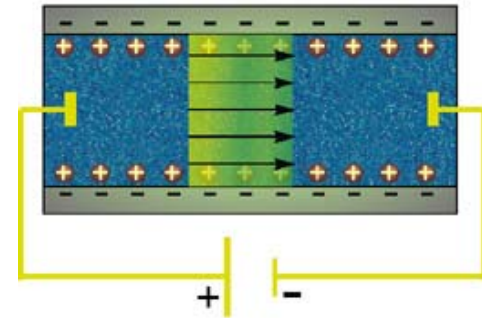
Electric -> Hydrodynamic



3.7.2. Electroosmotic Flow

- Mechanism

- „Reversed streaming“
- EDL
- Axial electric field, tangential to surface
- Force on net charge in diffuse mobile layer
- Bulk fluid dragged by mobile layer like „chains“
- Negative surface charges
 - EOF towards cathode



$$\mathbf{f}_q(\mathbf{x}) = \rho_q(\mathbf{x}) \mathbf{E}(\mathbf{x})$$

- Electroosmotic mobility

- Electric field $E = U/l$
- Equation of motion (NS)
 - Steady flow of incompressible fluid at low Re
- Helmholtz-Smoluchowski relation
 - Limit of small Debye length
- EO mobility
 - Not EP mobility
 - ζ -potential
 - Viscosity η

$$-\nabla p + \eta \nabla^2 \mathbf{v} - \rho_q \mathbf{E} = 0$$

$$v_\zeta = \mu_\zeta |E|$$

$$\mu_\zeta = \frac{\varepsilon \varepsilon_0 \zeta}{\eta}$$

3.7.2. Flow Profile

- Velocity field

$$\nabla \cdot \mathbf{E} = \frac{1}{\epsilon_0} \rho_q(\mathbf{r}, t)$$

- Assumption: $v \sim E$
- v-profile directly from Poisson
- v-profile roughly follows potential ψ across capillary
 - Strong variation only near wall
 - Immobilized Stern layer: $v = 0$
 - V_{\max} reached at shear layer
 - Flat profile in center at value $v = v_\zeta$
 - Plug-like shape

$$v = \mu_\zeta |\mathbf{E}| \left(1 - \frac{\psi(r)}{\zeta} \right)$$

$\psi(0) = 0, \psi(r) \mapsto 0$ at $r \gg r_D$

- Dependency ψ / ζ mostly negligible

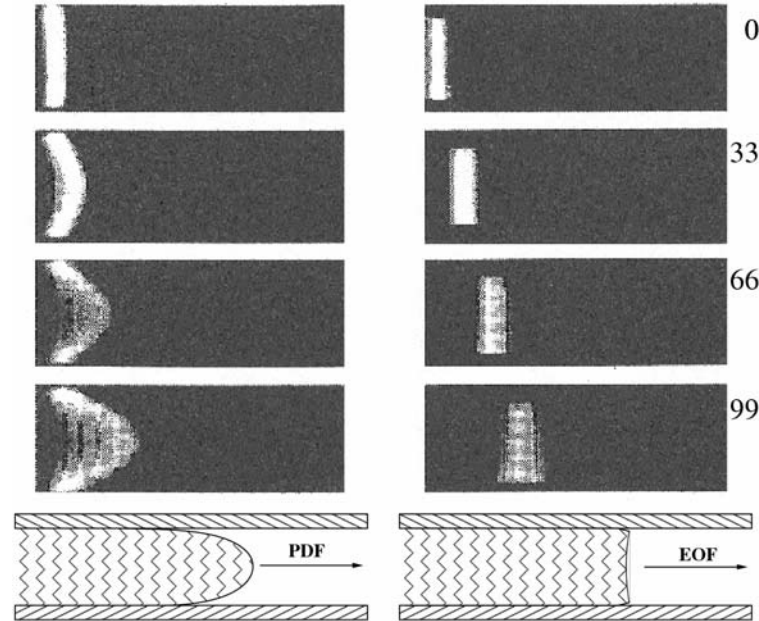


Fig. 3.42. Velocity profiles in pressure-driven and electroosmotic flow and experimental observations recorded in 33-ms time frames

3.7.2. Pressure Gradient

- Pressure difference counteracting EOF
- Superposition of PDF and EOF profile
 - Cylindrical channel
 - Length l

$$v_z(r) = \frac{p}{4\eta l} (r_0^2 - r^2) - \frac{\epsilon\epsilon_0\zeta U}{\eta l}$$

- Parallel plates
 - Gap distance d parabolic flat

$$v_z(r) = \frac{p}{2\eta l} \left(\frac{d^2}{4} - y^2 \right) - \frac{\epsilon\epsilon_0\zeta U}{\eta l}$$

3.7.2. Temporal Evolution of EOF

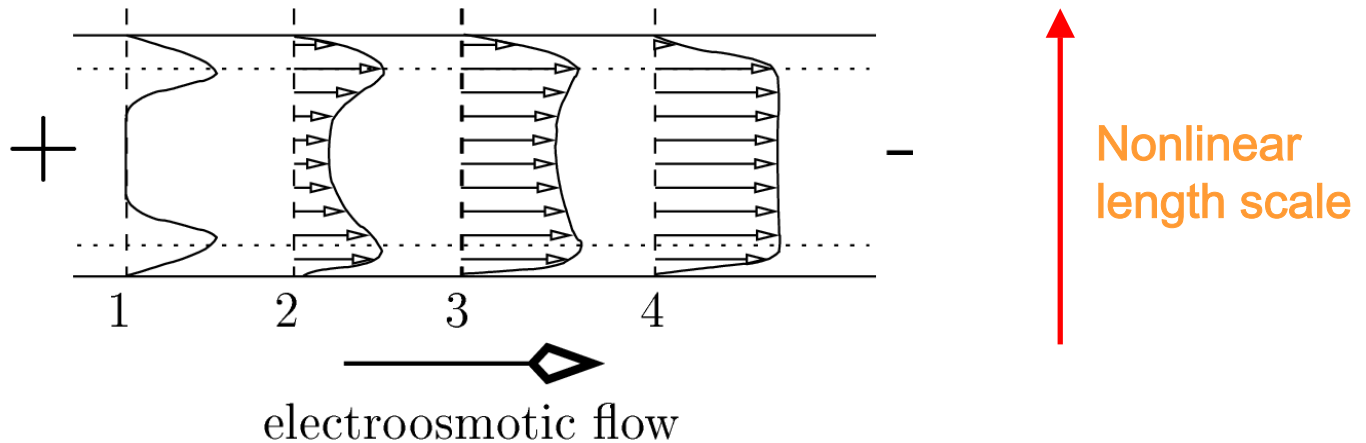
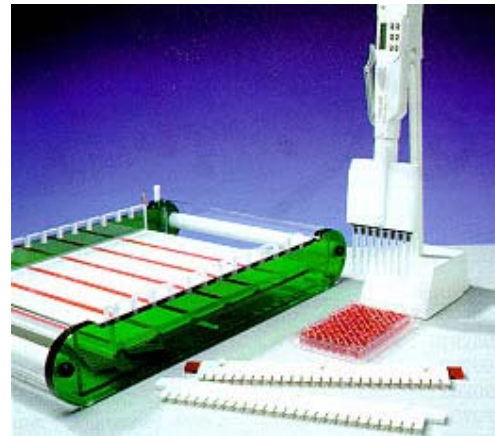


Fig. 3.43. Evolution of EOF from the switching of the external field (left) to a fully developed flow (right) where hydrated charges from the diffuse layer mediate the flow by viscous drag

- No „dispersion“ of EOF plug
 - Broadening widely suppressed
- Charged layer pulled by electric field
 - Bulk liquid dragged along

3.7. Electrokinetics

1. Electric Double Layers
2. Electroosmotic Flow
- 3. Electrophoresis**
4. Dielectrophoresis



3.7.3. Electrophoresis

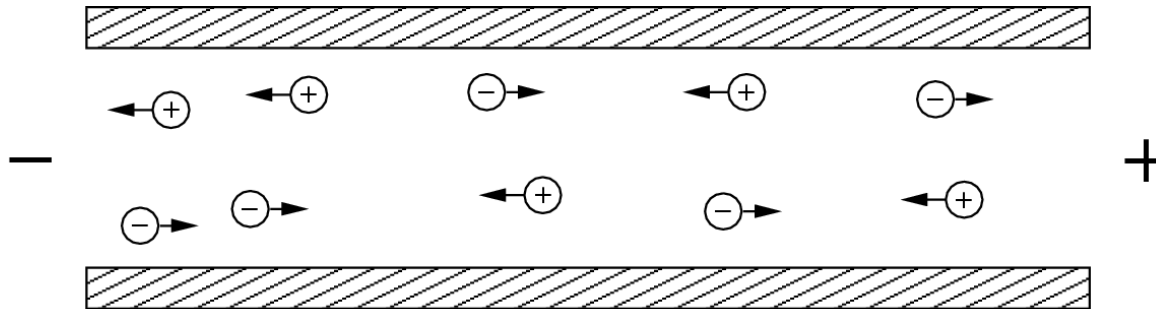


Fig. 3.44. Migration of ions in electrophoresis

- Ionic mobility μ_i
 - Electric field strength $|\mathbf{E}|$
 - Velocity of ions \mathbf{v}_i
- Electrophoresis
 - Method in analytical chemistry
 - Separation according to μ_i
- Kohlrausch's law
 - Limit of high dilution
 - Independent migration of ions

$$\begin{aligned}v_+ &= \mu_+ |\mathbf{E}| \\v_- &= -\mu_- |\mathbf{E}|\end{aligned}$$

$$\mu = \frac{el_{\text{mfp}}}{2mv_T}$$

3.7.3. Electrophoresis

- Electrophoretic (ionic) mobility
 - Governed by charge-to-size ratio
 - Charge
 - Electric “pull” force
 - Size
 - Frictional drag with bulk molecules
- Stokes model
 - Molecular structure approximated by sphere
 - Radius r_i
 - Charge q_i
 - Stokes drag: $F_{\text{Stokes}} = q |\mathbf{E}|$
 - Balanced by electric field
 - Viscosity η
 - Background electrolyte

$$\mu_i = \frac{v_i}{|\mathbf{E}|} = \frac{q_i}{6\pi\eta r_i}$$

- Electrophoretic speed usually much smaller than EOF!

3.7.3. Joule Heating

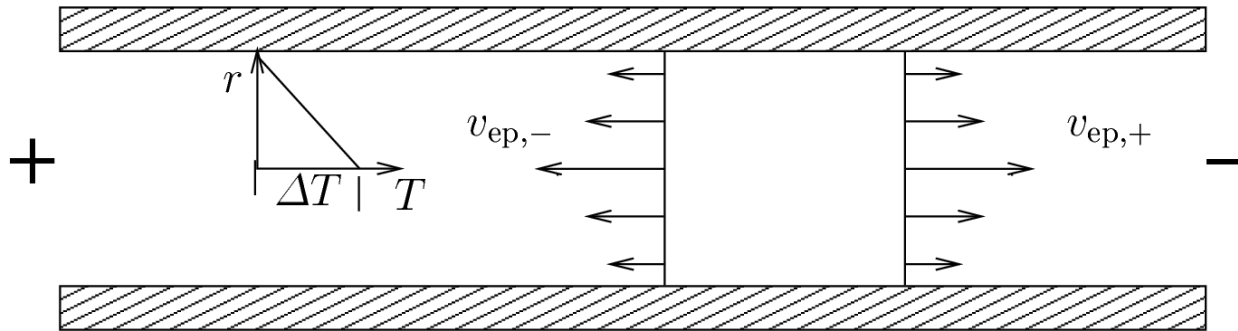


Fig. 3.45. Joule heating induces a temperature difference ΔT which leads to a nonuniform profile of the electrophoretic velocities $v_{ep,i}$

- Speed of electrophoretic motion / separation
 - Grows with field strength $E = U / l$
- Electrolyte
 - Ohmic resistor
 - Dissipation of energy
 - Heating of liquid
 - Temperature gradient

3.7.3. Joule Heating

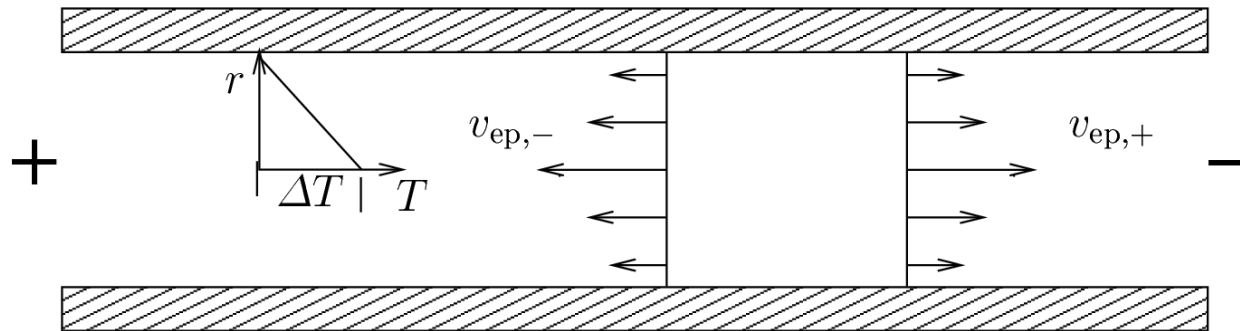


Fig. 3.45. Joule heating induces a temperature difference ΔT which leads to a nonuniform profile of the electrophoretic velocities $v_{ep,i}$

- Rate of heat generation

$$P_Q = \frac{dE}{dt} = \frac{U^2}{R} = \frac{\sigma_E A U^2}{l} = \sigma_E A l |E|^2$$

- Square of field strength $|E|^2$
- Capillary length l

- Temperature drop

- Cylindrical capillary
- Decreases with **radius**

$$\Delta T \propto \frac{P_Q r_{cap}^2}{\lambda}$$

3.7.3. Joule Heating – Temperature Gradient

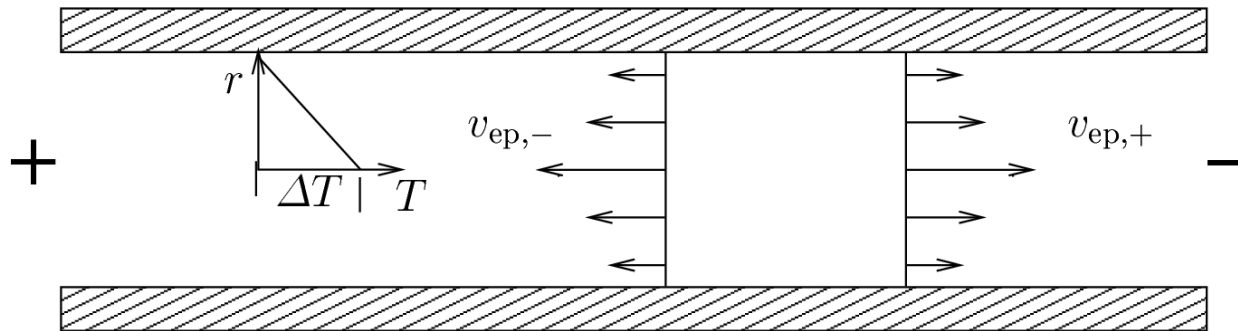


Fig. 3.45. Joule heating induces a temperature difference ΔT which leads to a nonuniform profile of the electrophoretic velocities $v_{ep,i}$

- Band broadening by viscosity
 - **Viscosity** η decreases with T
 - **Effective ion radius** r (hydration) shrinks
 - Enhanced **EP mobility** in hot areas
 - Approx. 2%-increase per Kelvin
 - Flow profile resembles PDF profile
 - Solutions

$$\Delta T \propto \frac{P_Q r_{\text{cap}}^2}{\lambda}$$

$$\eta = \frac{k_B T}{a^3 \nu_0} \exp\left(\frac{E_0}{k_B T}\right)$$

$$\mu_i = \frac{v_i}{|\mathbf{E}|} = \frac{q_i}{6\pi\eta r_i}$$

3.7.3. Joule Heating – Temperature Gradient

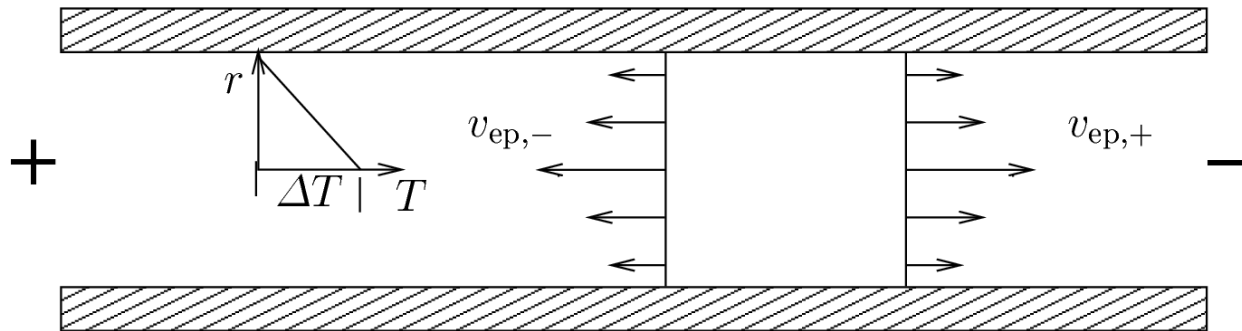


Fig. 3.45. Joule heating induces a temperature difference ΔT which leads to a nonuniform profile of the electrophoretic velocities $v_{ep,i}$

- Band broadening by buoyancy

- Temperature gradient
- Free convection

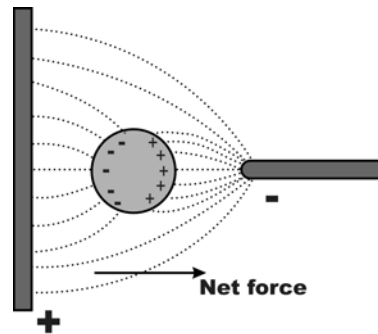
$$\Delta T \propto \frac{P_Q r_{\text{cap}}^2}{\lambda}$$

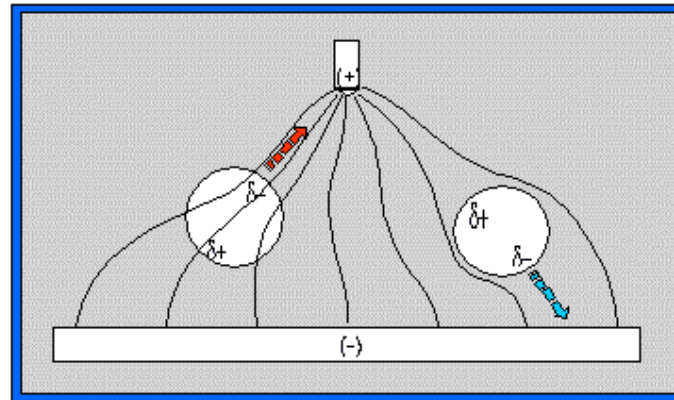
- Counter measures

- Small-diameter capillaries
 - Fast transport of heat from liquid to wall
- Cooled walls

3.7. Electrokinetics

1. Electric Double Layers
2. Electroosmotic Flow
3. Electrophoresis
- 4. Dielectrophoresis**





Two different particles in a non-uniform electric field. The particle on the left is more polarizable than the surrounding medium and is attracted towards the strong field at the pin electrode, whilst the particle of low polarizability on the right is directed away from the strong field region.

3.7.4. Dielectrophoresis

$$\mathbf{F}_E = [q + (\mathbf{p}_q \cdot \nabla)] \mathbf{E}$$

- Electric field
 - Monopole force
 - Charge q
 - Dipole term
 - Electric dipole moment $\mathbf{p}_q = q \mathbf{r}$
 - Inhomogeneous field $\text{grad } \mathbf{E} \neq 0$
- AC dielectrophoretic (DEP) force
 - Oscillating external field
 - Induced dipole moment
 - Phase lag
 - Particle motion
 - E -field

$$\mathbf{F}_{\text{DEP}} = \frac{\text{Re}[\mathbf{p}_q]}{2|\mathbf{E}|} \nabla (|\mathbf{E}|^2)$$

- Application in microfluidics
 - Separation / manipulation of large particles
 - Cells
 - Beads

3.7.4. Induced Dipole Moments

- Dielectric permittivity
 - Frequency of external field ν
 - Permittivities $\varepsilon_i(\nu)$
 - Particle
 - Surrounding medium
- Example: spherical particle
 - Radius r_0
 - Clausius-Mossotti factor f_ε

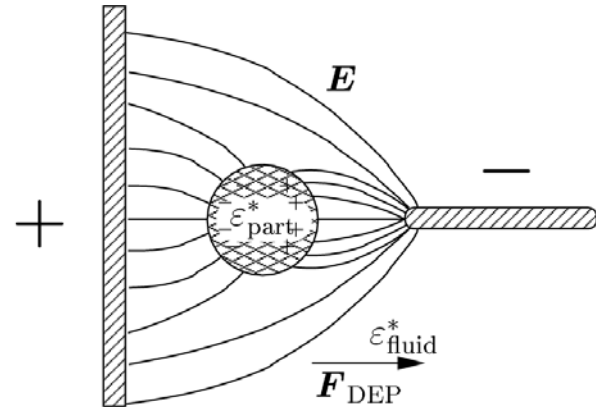


Fig. 3.46. Dielectric forces experienced by a polarizable particle in an inhomogeneous electric field ($\nabla E \neq 0$)

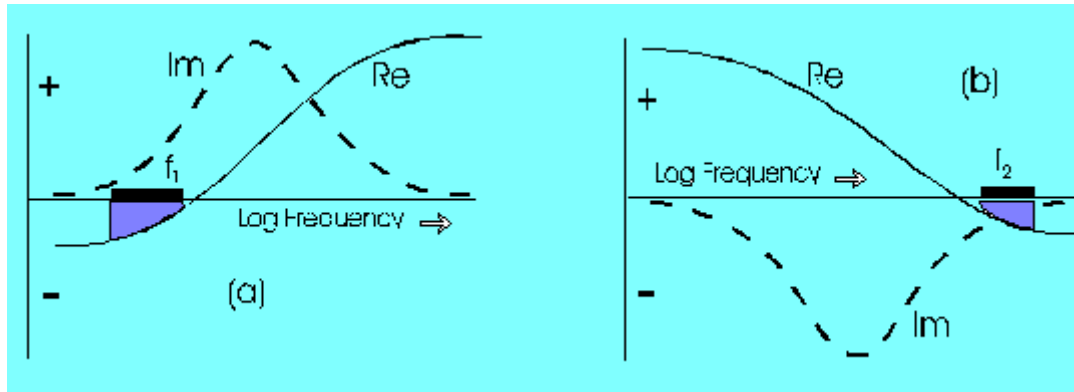
$$\mathbf{p}_q(\nu) = 4\pi\varepsilon_0\varepsilon_{\text{fluid}} f_\varepsilon(\varepsilon_{\text{part}}^*, \varepsilon_{\text{fluid}}^*) r_0^3 \mathbf{E} = \alpha_\varepsilon(\nu) \mathbf{E}$$

$$f_\varepsilon(\varepsilon_{\text{part}}^*(\nu), \varepsilon_{\text{fluid}}^*(\nu)) = \frac{\varepsilon_{\text{part}}^*(\nu) - \varepsilon_{\text{fluid}}^*(\nu)}{\varepsilon_{\text{part}}^*(\nu) + 2\varepsilon_{\text{fluid}}^*(\nu)}$$

- Induced force

$$\mathbf{F}_{\text{DEP}} = 2\pi\varepsilon_0\varepsilon_{\text{fluid}} \text{Re}[f_\varepsilon(\varepsilon_{\text{part}}^*(\nu), \varepsilon_{\text{fluid}}^*(\nu))] r_0^3 \nabla (|\mathbf{E}|^2)$$

3.7.4. Induced Dipole Moments



- Frequency variations of the real and imaginary components of the induced dipole moment for model cases of (a) a viable cell with an intact membrane, and (b) a cell with a porous membrane. Translational motion under the influence of traveling fields can occur in frequency ranges f_1 and f_2 .

3.7.3. Positive & Negative DEP



3.7.4. Cell Separation

- Array of interdigitated electrodes
- Force depends on
 - Permittivities
 - RMS voltage U
 - Geometry / setup (inhomogeneous field)

$$F_{\text{DEP}} = 1.5V \varepsilon_{\text{fluid}} \alpha_{\text{DEP}}(\nu) U^2 \beta^2(\nu) A e^{-2\pi h/d}$$

- Field-induced dielectrophoretic polarizability

$$\alpha_{\text{DEP}} = \text{Re} \left[\frac{\varepsilon_{\text{cell}}^*(\nu) - \varepsilon_{\text{fluid}}^*(\nu)}{3(\varepsilon_{\text{cell}}^*(\nu) - \varepsilon_{\text{fluid}}^*(\nu))A_i + 3\varepsilon_{\text{fluid}}^*(\nu)} \right]$$

- Excentricity A_i

- Permittivity of cell

- Internal
- Membrane

$$\varepsilon_{\text{cell}}^* = \varepsilon_{\text{mem}}^* \frac{\varepsilon_{\text{mem}}^* + \frac{\varepsilon_{\text{int}}^* - \varepsilon_{\text{mem}}^*}{A_i + \hat{V}(1 - A_i)}}{\varepsilon_{\text{mem}}^* + \frac{\varepsilon_{\text{int}}^* - \varepsilon_{\text{mem}}^*}{A_i - \hat{V}A_i}}$$

3.7.4. Traveling-Wave DEP

- Linear analogue of electrorotation
 - Linear arrangement of electrodes
 - 90° phase shift between electrodes

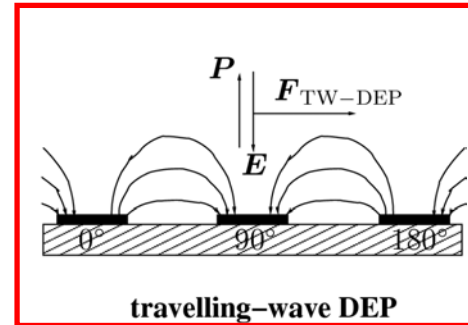
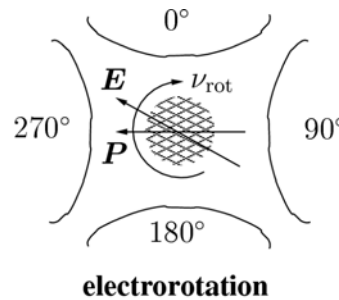


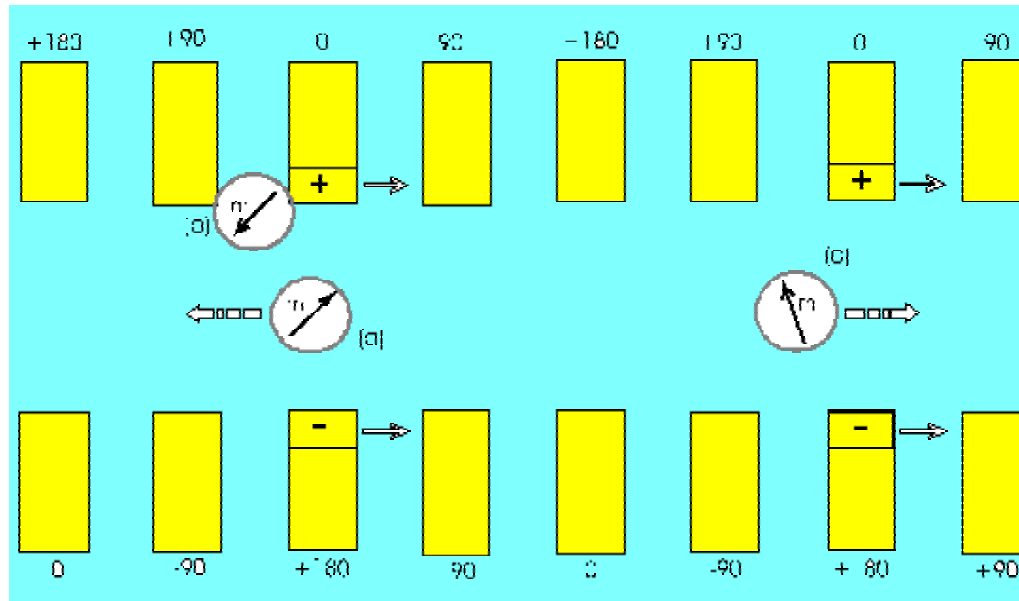
Fig. 3.47. Electrorotation (left) and travelling wave DEP (right)

- Force on particle

$$F_{\text{TW-DEP}} = - \frac{4\pi\epsilon_0\epsilon_{\text{fluid}}\epsilon r_0^3 \text{Im}[f_\epsilon(\nu)] |\mathbf{E}|^2}{\lambda}$$

- Wave length of traveling field λ

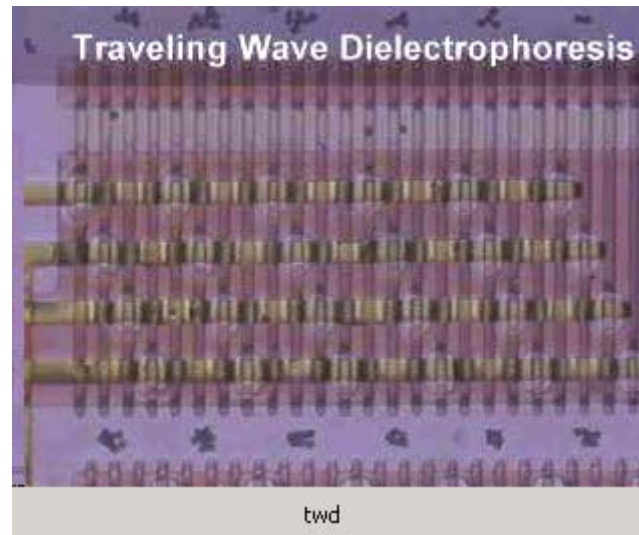
3.7.4. Traveling-Wave DEP



An electric "wave" traveling from left to right is produced by electrodes of this design if energized by cosine voltages of the indicated phase relationships. (a) Motion expected for a viable cell (f_1 in Figure 2). (b) A cell trapped by positive dielectrophoresis. (c) Motion of a non-viable cell.

3.7.4. Traveling-Wave DEP

IBMM



3.7.4. Electrorotation

- DEP in rotating dipole field
 - Polarizable particle suspended in rotating field

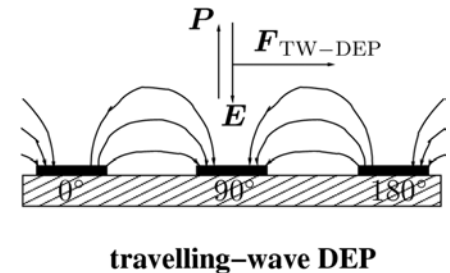
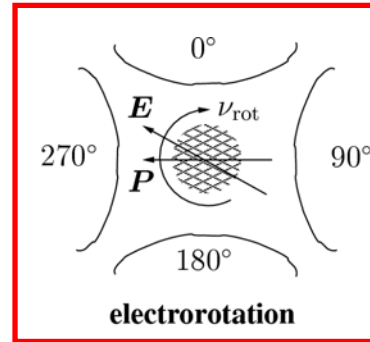


Fig. 3.47. Electrorotation (left) and travelling wave DEP (right)

- Torque on particle
 - Sufficient angular velocities
 - Rotation of dipole lags field
 - Frequency-dependent phase shift
 - Geometrical angle between \mathbf{E} and \mathbf{p}_q

$$[\tau] = -4\pi\epsilon_0\epsilon_{\text{fluid}}\epsilon r_0^3 \text{Im}[f_\epsilon(\nu)] |\mathbf{E}|^2$$